nature

https://doi.org/10.1038/s41586-021-04231-6

Accelerated Article Preview

Optimization of Non-Coding Regions for a Non-Modified mRNA COVID-19 Vaccine

Received: 13 August 2021

Accepted: 11 November 2021

Accelerated Article Preview Published online 18 November 2021

Cite this article as: Gebre, M. S. et al. Optimization of Non-Coding Regions for a Non-Modified mRNA COVID-19 Vaccine. *Nature* https://doi.org/10.1038/s41586-021-04231-6 (2021).

Makda S. Gebre, Susanne Rauch, Nicole Roth, Jingyou Yu, Abishek Chandrashekar, Noe B. Mercado, Xuan He, Jinyan Liu, Katherine McMahan, Amanda Martinot, David R. Martinez, Tori Giffin, David Hope, Shivani Patel, Daniel Sellers, Owen Sanborn, Julia Barrett, Xiaowen Liu, Andrew C. Cole, Laurent Pessaint, Daniel Valentin, Zack Flinchbaugh, Jake Yalley-Ogunro, Jeanne Muench, Renita Brown, Anthony Cook, Elyse Teow, Hanne Andersen, Mark G. Lewis, Adrianus C. M. Boon, Ralph S. Baric, Stefan O. Mueller, Benjamin Petsch & Dan H. Barouch

Optimization of Non-Coding Regions for a Non-Modified mRNA COVID-19 Vaccine

https://doi.org/10.1038/s41586-021-04231-6

Received: 13 August 2021

Accepted: 11 November 2021

Published online: 18 November 2021

Makda S. Gebre[1,9], Susanne Rauch[2,9]✉, Nicole Roth[2], Jingyou Yu[1], Abishek Chandrashekar[1], Noe B. Mercado[1], Xuan He[1], Jinyan Liu[1], Katherine McMahan[1], Amanda Martinot[3], David R. Martinez[4], Tori Giffin[1], David Hope[1], Shivani Patel[1], Daniel Sellers[1], Owen Sanborn[1], Julia Barrett[1], Xiaowen Liu[5], Andrew C. Cole[5], Laurent Pessaint[6], Daniel Valentin[6], Zack Flinchbaugh[6], Jake Yalley-Ogunro[6], Jeanne Muench[6], Renita Brown[6], Anthony Cook[6], Elyse Teow[6], Hanne Andersen[6], Mark G. Lewis[6], Adrianus C. M. Boon[7], Ralph S. Baric[4], Stefan O. Mueller[2], Benjamin Petsch[2,9] & Dan H. Barouch[1,8,9]✉

The CVnCoV (CureVac) mRNA vaccine for SARS-CoV-2 has recently been evaluated in a phase 2b/3 efficacy trial in humans[1]. CV2CoV is a second-generation mRNA vaccine with non-modified nucleosides but optimized non-coding regions and enhanced antigen expression. Here we report a head-to-head study of the immunogenicity and protective efficacy of CVnCoV and CV2CoV in nonhuman primates. We immunized 18 cynomolgus macaques with two doses of 12 ug of lipid nanoparticle formulated CVnCoV, CV2CoV, or sham (N=6/group). CV2CoV induced substantially higher binding and neutralizing antibodies, memory B cell responses, and T cell responses as compared with CVnCoV. CV2CoV also induced more potent neutralizing antibody responses against SARS-CoV-2 variants, including the delta variant. Moreover, CV2CoV proved comparably immunogenic to the BNT162b2 (Pfizer) vaccine in macaques. While CVnCoV provided partial protection against SARS-CoV-2 challenge, CV2CoV afforded more robust protection with markedly lower viral loads in the upper and lower respiratory tract. Binding and neutralizing antibody titers correlated with protective efficacy. These data demonstrate that optimization of non-coding regions can greatly improve the immunogenicity and protective efficacy of a non-modified mRNA SARS-CoV-2 vaccine in nonhuman primates.

The CVnCoV mRNA vaccine (CureVac) has recently reported efficacy results in humans in the Phase 2b/3 HERALD trial in a population that included multiple viral variants. The observed vaccine efficacy against symptomatic COVID-19 was approximately 48% and 53% in the overall study population and in the 18-60 years of age subgroup, respectively[1]. CV2CoV is a second-generation mRNA vaccine that involves modifications of the non-coding regions that were selected based on an empiric screen for improved antigen expression[2,3]. Both CVnCoV and CV2CoV are based on RNActive® technology[4–7] and consist of non-chemically modified, sequence engineered mRNA without pseudouridine[6–12]. Both vaccines encode for the same full-length, pre-fusion stabilized SARS-CoV-2 spike (S)[13,14] and are encapsulated in lipid nanoparticles (LNP) with identical composition. CV2CoV has been engineered with different non-coding regions flanking the open reading frame, which have previously been shown to improve transgene expression[3] and protection against SARS-CoV-2 in ACE2 transgenic mice[2]. Specifically, CV2CoV includes 5′ UTR HSD17B4 and 3′ UTR PSMB3 elements, followed by a histone stem loop motif and a poly-A sequence (Fig. 1; see Methods). In this study, we compare head-to-head the immunogenicity and protective efficacy of CVnCoV and CV2CoV against SARS-CoV-2 challenge in nonhuman primates.

Vaccine Immunogenicity

We immunized 18 cynomolgus macaques intramuscularly with 12 µg CVnCoV, 12 µg CV2CoV, or sham vaccine (Fig. 1b). Animals were primed at week 0 and boosted at week 4. No clinical adverse effects were observed following vaccination. To assess innate immune responses, sera was isolated from all animals 24h after the first vaccination to assess innate cytokine responses. CV2CoV induced higher levels of IFNα2a, IP-10 and MIP-1 compared with CVnCoV ($P = 0.0152$, $P = 0.0152$, $P = 0.0411$, respectively; Extended Data Fig. 1).

Binding antibody responses were assessed by receptor binding domain (RBD)-specific ELISAs at multiple timepoints following immunization[15,16]. At week 2, binding antibody titers were only detected with CV2CoV and not with CVnCoV (CVnCoV median titer 25 [range 25-25]; CV2CoV median titer 799 [range 82-2,010]) (Fig. 2a). One week following the week 4 boost, antibody titers increased in both groups (CVnCoV

[1]Center for Virology and Vaccine Research, Beth Israel Deaconess Medical Center, Harvard Medical School, Boston, MA, 02215, USA. [2]CureVac AG, Tübingen, Germany. [3]Tufts University Cummings School of Veterinary Medicine, North Grafton, MA, USA. [4]University of North Carolina at Chapel Hill, Chapel Hill, NC, USA. [5]Department of Emergency Medicine, Beth Israel Deaconess Medical Center, Boston, MA, 02215, USA. [6]Bioqual, Rockville, MD, 20852, USA. [7]Department of Internal Medicine, Washington University School of Medicine, Saint Louis, MO, USA. [8]Ragon Institute of MGH, MIT and Harvard, Cambridge, MA, USA. [9]These authors contributed equally: Makda S. Gebre, Susanne Rauch, Benjamin Petsch, Dan H. Barouch.
✉e-mail: Susanne.rauch@curevac.com; dbarouch@bidmc.harvard.edu

median titer 48 [range 75-710]); CV2CoV median titer 28,407 [range 2,714-86,541]) (Fig. 2a). By week 8, binding antibody titers increased in the CVnCoV group but were still >50-fold lower than in the CV2CoV group (P=0.0043) (CVnCoV median titer 214 [range 47-1,238]; CV2CoV median titer 14,827 [range 2,133-37,079]).

Neutralizing antibody (NAb) responses were assessed by pseudovirus neutralization assays using the vaccine-matched SARS-CoV-2 wildtype (WT) WA1/2020 strain[15–17]. NAb titers followed a similar trend as binding antibody titers (Fig. 2b). At week 2, NAb were only detected with CV2CoV and not with CVnCoV (CVnCoV median titer 20 [range 20-20]; CV2CoV median titer 131 [range 62-578]) (Fig. 2b). One week following the week 4 boost, NAb titers increased (CVnCoV median titer 55 [range 20-302]; CV2CoV median titer 15,827 [range 3,985-81,081]). By week 8, NAb titers increased in the CVnCoV group but were still >20-fold lower than in the CV2CoV group (P=0.0022) (CVnCoV median titer 196 [range 20-405]; CV2CoV median titer 4,752 [range 414-6,793]).

At week 6, median NAb titers against the D614G, B.1.1.7 (alpha), and B.1.351 (beta) variants were 121, 101, and 189, respectively, for CVnCoV and were 4,962, 1,813, and 755, respectively, for CV2CoV (Fig. 2c). Median NAb titers against C.37 (lambda), B.1.617.1 (kappa), and B.1.617.2 (delta) were 516, 158, and 36, respectively, for CVnCoV and were 1195, 541, and 568, respectively, for CV2CoV (Extended Data Fig. 2). NAb titers induced by CV2CoV were higher than CVnCoV for the WT (WA1/2020), D614G, B.1.1.7 (alpha), B.1.351 (beta), C.37 (lambda), B.1.617.1 (kappa), and B.1.617.2 (delta) strains (P=0.0043, 0.0087, 0.0043, 0.1320, 0.026, 0.0022, and 0.0043, respectively). Taken together, these data show that CV2CoV induced substantially higher NAb titers against SARS-CoV-2 variants compared with CVnCoV.

Live-virus NAb titers[18] were largely consistent with pseudovirus NAb titers. Live virus NAb responses elicited by CV2CoV were higher than CVnCoV against the WA1/2020 and B.1.617.2 (delta) variants (P=0.0466 and P=0.0152, respectively), with similar trends for B.1.1.7 (alpha) and B.1.351 (beta) (P=0.0628 and 0.1450, respectively) (Fig. 2d).

We also compared pseudovirus NAb titers induced in macaques by 2 immunizations of 12 ug of CV2CoV with 2 immunizations of 30 ug of the Pfizer BNT162b2 clinical vaccine, which was leftover vaccine obtained from pharmacies. At peak immunity at week 5, NAb responses induced by CV2CoV were comparable to NAb responses induced by BNT162b2 (Fig. 2e).

Most SARS-CoV-2 RBD-specific B cells reside within the memory B cell pool[19]. We assessed memory B cell responses in blood from CVnCoV, CV2CoV and sham vaccinated NHPs by flow cytometry[20]. Higher RBD- and spike-specific memory B cells were detected in CV2CoV vaccinated animals compared with CVnCoV vaccinated animals at week 6 (P=0.022, P=0.0152, respectively) (Extended Data Fig. 3a, b). T cell responses were assessed by IFN-γ and IL-4 enzyme-linked immunosorbent spot (ELISPOT) assay using pooled S peptides at week 6. IFN-γ responses were detected in both groups but were higher in the CV2CoV group (P=0.0065) (Extended Data Fig. 3c). IL-4 responses were not detectable, suggesting that CVnCoV and CV2CoV induced Th1 biased responses (Extended Data Fig. 3d).

Protective Efficacy

All animals were challenged at week 8 with 1.0×10^5 $TCID_{50}$ SARS-CoV-2 WA1/2020 strain via the intranasal (IN) and intratracheal (IT) routes. Viral loads were assessed in bronchoalveolar lavage (BAL) and nasal swab (NS) samples collected on days 1, 2, 4, 7 and 10 following challenge by RT-PCR specific for subgenomic RNA (sgRNA)[21]. Subgenomic RNA levels in BAL and NS in the sham group peaked on day 2 and largely resolved by day 10. Sham controls had a peak median of 6.02 (range 4.62–6.81) log_{10} sgRNA copies/ml in BAL and 7.35 (range 5.84–8.09) log_{10} sgRNA copies/swab in NS on day 2 (Fig. 3). CVnCoV immunized animals showed a peak median of 4.92 (range 2.40–6.61) log_{10} sgRNA copies/ml in BAL and 6.42 (range 4.46–7.81) log_{10} sgRNA copies/swab in NS (Fig. 3). CV2CoV immunized animals exhibited a peak median of 2.90 (range 1.70–4.64) log_{10} sgRNA copies/ml in BAL and 3.17 (range 2.59–5.63) log_{10} sgRNA copies/swab in NS (Fig. 3), with resolution of sgRNA in BAL by day 2 in most animals and by day 4 in all animals. Overall, CV2CoV resulted in significantly lower peak viral loads than CVnCoV in both BAL (P=0.0411) and NS (P=0.0087) (Fig. 4a and b).

We next evaluated immune correlates of protection in this study. The log_{10} ELISA and NAb titers at week 6 inversely correlated with peak log_{10} sgRNA copies/ml in BAL (P=0.0008, R=−0.7148 and P=0.0015, R= −0.6912, respectively, two-sided Spearman rank-correlation test) (Fig. 4c, e) and with peak sgRNA copies/nasal swab in NS (P<0.0001, R=−0.8346, and P<0.0001, R=−0.8766, respectively, two-sided Spearman rank-correlation test) (Fig. 4d, f). Consistent with prior observations from our laboratory and others[15,16,22], these findings suggest that binding and neutralizing antibody titers are important correlates of protection for these SARS-CoV-2 vaccines in nonhuman primates. Similar correlates of protection were observed with viral loads assessed as area under the curve (AUC) (Extended Data Fig. 4). We also assessed infectious virus titers by $TCID_{50}$ assays on day 2 post challenge, which showed no detectable virus in 5 of 6 animals in the CV2CoV group (Extended Data Fig. 5).

Following challenge, we observed anamnestic binding and neutralizing antibody responses in all the CVnCoV vaccinated animals and in a subset of the CV2CoV vaccinated animals[16] (Extended Data Fig. 6). On day 10 post-challenge, animals were necropsied, and lung tissues were evaluated by histopathology. Viral replication had largely resolved by day 10 in CVnCoV and CV2CoV vaccinated animals, and sham animals had higher cumulative lung pathology scores[20] (CVnCoV animals P=0.0368, CV2CoV animals P=0.0022, compared with sham controls) (Extended Data Fig. 7a). Sham animals also had more lung lobes affected (Extended Data Fig. 7b) and more extensive lung lesions with a greater proportion of lung lobes showing evidence of interstitial inflammation, alveolar inflammatory infiltrates, and type II pneumocyte hyperplasia (Extended Data Fig. 7c–h). No significant eosinophilia was observed. Pathologic lesions in vaccinated animals were similar to those observed in sham animals (Extended Data Fig. 7i–l) but fewer overall and more focal in distribution.

Discussion

CV2CoV elicited substantially higher humoral and cellular immune responses and provided significantly improved protective efficacy against SARS-CoV-2 challenge compared with CVnCoV in macaques. These data suggest that optimization of non-coding elements of the mRNA backbone can substantially improve the immunogenicity and protective efficacy of mRNA vaccines. Both CVnCoV and CV2CoV contain only non-modified nucleosides, without pseudouridine or derivates, and CV2CoV has previously been shown to lead to higher antigen expression than CVnCoV in cell culture[3]. NAb titers induced by CV2CoV were comparable in macaques to NAb titers induced by the clinical BNT162b2 vaccine, which includes pseudouridine, suggesting that strategies other than nucleoside modification can also markedly improve mRNA potency.

While previous studies in rodents and nonhuman primates have demonstrated protection by CVnCoV[2,23,24], this was only studied in the lower respiratory tract[24]. In the present study, CVnCoV provided only modest reductions in viral loads in BAL and NS compared with sham controls. In contrast, CV2CoV induced >10-fold higher NAb responses than CVnCoV against multiple viral variants and provided >3 log reductions in sgRNA copies/ml in BAL and >4 log reductions in sgRNA copies/swab in NS compared with sham controls.

Previous mRNA vaccine clinical trials have demonstrated onset of protective efficacy after the first dose and improved protection after the boost immunization[25,26]. In the present study, the prime immunization with CV2CoV induced binding and neutralizing antibodies in all

macaques by week 2, and these responses increased substantially by 1 week after the boost immunization. NAb titers induced by CV2CoV in this study also appear similar to NAb titers reported for other mRNA vaccines in macaques[27,28]. Moreover, NAb titers induced by BNT162b2 in our study (Fig. 2e) were comparable to NAb titers reported for BNT162b2 in a prior study[28].

As previously reported for other vaccines[29–33], NAb titers were lower to certain SARS-CoV-2 variants, including B.1.351 (beta) and B.1.617.2 (delta), than to the parental strain WA1/2020. Although our challenge virus in this study was SARS-CoV-2 WA1/2020, NAb titers elicited by CV2CoV to these viral variants exceeded the threshold that we previously reported as threshold titers for protection (50-100)[17,20,22]. However, future studies will be required to assess directly the protective efficacy of CV2CoV against SARS-CoV-2 variants of concern in non-human primates.

CV2CoV induced both antigen-specific memory B cell responses and T cell responses. While the correlates of protection in this study were binding and neutralizing antibodies[34,35], it is likely that $CD8^+$ T cells contribute to viral clearance in tissues[36,37]. We previously reported that depletion of $CD8^+$ T cells partially abrogated protective efficacy against SARS-CoV-2 re-challenge in convalescent macaques[22]. Memory B cells may contribute to durability of antibody responses[38,39], although B cell germinal center responses and durability of protective efficacy following CV2CoV vaccination remain to be determined. Moreover, although this study was not specifically designed as a safety study, it is worth noting that we did not observe any adverse effects following CVnCoV or CV2CoV vaccination, and we did not observe any unexpected or enhanced pathology in the vaccinated animals at necropsy[40].

In summary, our data show that optimization of non-coding regions in a SARS-CoV-2 mRNA vaccine can substantially improve its immunogenicity against multiple viral variants and enhance protective efficacy against SARS-CoV-2 challenge in macaques. Improved characteristics of CV2CoV, compared with CVnCoV, may translate into increased efficacy in humans, and clinical trials of CV2CoV are planned.

Online content

Any methods, additional references, Nature Research reporting summaries, source data, extended data, supplementary information, acknowledgements, peer review information; details of author contributions and competing interests; and statements of data and code availability are available at https://doi.org/10.1038/s41586-021-04231-6.

1. Peter G. et al. Efficacy and Safety of the CVnCoV SARS-CoV-2 mRNA Vaccine Candidate: Results from Herald, a Phase 2b/3, Randomised, Observer-Blinded, Placebo-Controlled Clinical Trial in Ten Countries in Europe and Latin America. *The Lancet (Preprint)* (2021).
2. Hoffmann, D. et al. CVnCoV and CV2CoV protect human ACE2 transgenic mice from ancestral B BavPat1 and emerging B.1.351 SARS-CoV-2. *Nat Commun* **12**, 4048, https://doi.org/10.1038/s41467-021-24339-7 (2021).
3. Nicole Roth, J. S. et al. CV2CoV, an enhanced mRNA-based SARS-CoV-2 vaccine candidate, supports higher protein expression and improved immunogenicity in rats. *bioRxiv* (2021).
4. Hoerr, I., Obst, R., Rammensee, H. G. & Jung, G. In vivo application of RNA leads to induction of specific cytotoxic T lymphocytes and antibodies. *Eur J Immunol* **30**, 1-7, 10.1002/1521-4141(200001)30:1<1::AID-IMMU1>3.0.CO;2-# (2000).
5. Fotin-Mleczek, M. et al. Highly potent mRNA based cancer vaccines represent an attractive platform for combination therapies supporting an improved therapeutic effect. *J Gene Med* **14**, 428-439, https://doi.org/10.1002/jgm.2605 (2012).
6. Fotin-Mleczek, M. et al. Messenger RNA-based vaccines with dual activity induce balanced TLR-7 dependent adaptive immune responses and provide antitumor activity. *J Immunother* **34**, 1-15, https://doi.org/10.1097/CJI.0b013e3181f7dbe8 (2011).
7. Kubler, H. et al. Self-adjuvanted mRNA vaccination in advanced prostate cancer patients: a first-in-man phase I/IIa study. *J Immunother Cancer* **3**, 26, https://doi.org/10.1186/s40425-015-0068-y (2015).
8. Lutz, J. et al. Unmodified mRNA in LNPs constitutes a competitive technology for prophylactic vaccines. *NPJ Vaccines* **2**, 29, https://doi.org/10.1038/s41541-017-0032-6 (2017).
9. Stitz, L. et al. A thermostable messenger RNA based vaccine against rabies. *PLoS Negl Trop Dis* **11**, e0006108, https://doi.org/10.1371/journal.pntd.0006108 (2017).
10. Schnee, M. et al. An mRNA Vaccine Encoding Rabies Virus Glycoprotein Induces Protection against Lethal Infection in Mice and Correlates of Protection in Adult and Newborn Pigs. *PLoS Negl Trop Dis* **10**, e0004746, https://doi.org/10.1371/journal.pntd.0004746 (2016).
11. Petsch, B. et al. Protective efficacy of in vitro synthesized, specific mRNA vaccines against influenza A virus infection. *Nat Biotechnol* **30**, 1210-1216, https://doi.org/10.1038/nbt.2436 (2012).
12. Aldrich, C. et al. Proof-of-concept of a low-dose unmodified mRNA-based rabies vaccine formulated with lipid nanoparticles in human volunteers: A phase 1 trial. *Vaccine* **39**, 1310-1318, https://doi.org/10.1016/j.vaccine.2020.12.070 (2021).
13. Pallesen, J. et al. Immunogenicity and structures of a rationally designed prefusion MERS-CoV spike antigen. *Proc Natl Acad Sci U S A* **114**, E7348-E7357, https://doi.org/10.1073/pnas.1707304114 (2017).
14. Kirchdoerfer, R. N. et al. Stabilized coronavirus spikes are resistant to conformational changes induced by receptor recognition or proteolysis. *Sci Rep* **8**, 15701, https://doi.org/10.1038/s41598-018-34171-7 (2018).
15. Yu, J. et al. DNA vaccine protection against SARS-CoV-2 in rhesus macaques. *Science* **369**, 806-811, https://doi.org/10.1126/science.abc6284 (2020).
16. Mercado, N. B. et al. Single-shot Ad26 vaccine protects against SARS-CoV-2 in rhesus macaques. *Nature* **586**, 583-588, https://doi.org/10.1038/s41586-020-2607-z (2020).
17. Chandrashekar, A. et al. SARS-CoV-2 infection protects against rechallenge in rhesus macaques. *Science* **369**, 812-817, https://doi.org/10.1126/science.abc4776 (2020).
18. Martinez, D. R. et al. Chimeric spike mRNA vaccines protect against Sarbecovirus challenge in mice. *Science* **373**, 991-998, https://doi.org/10.1126/science.abi4506 (2021).
19. He, X. et al. Low-Dose Ad26.COV2.S Protection Against SARS-CoV-2 Challenge in Rhesus Macaques. *Cell*, https://doi.org/10.1016/j.cell.2021.05.040. (2021).
20. He, X. et al. Low-dose Ad26.COV2.S protection against SARS-CoV-2 challenge in rhesus macaques. *Cell* **184**, 3467-3473 e3411, https://doi.org/10.1016/j.cell.2021.05.040 (2021).
21. Dagotto, G. et al. Comparison of Subgenomic and Total RNA in SARS-CoV-2 Challenged Rhesus Macaques. *J Virol*, https://doi.org/10.1128/JVI.02370-20 (2021).
22. McMahan, K. et al. Correlates of protection against SARS-CoV-2 in rhesus macaques. *Nature* **590**, 630-634, https://doi.org/10.1038/s41586-020-03041-6 (2021).
23. Rauch, S. et al. mRNA-based SARS-CoV-2 vaccine candidate CVnCoV induces high levels of virus-neutralising antibodies and mediates protection in rodents. *NPJ Vaccines* **6**, 57, https://doi.org/10.1038/s41541-021-00311-w (2021).
24. Rauch, S., et al. mRNA vaccine CVnCoV protects non-human primates from SARS-CoV-2 challenge infection. *bioRxiv* (2020).
25. Polack, F. P. et al. Safety and Efficacy of the BNT162b2 mRNA Covid-19 Vaccine. *N Engl J Med* **383**, 2603-2615, https://doi.org/10.1056/NEJMoa2034577 (2020).
26. Baden, L. R. et al. Efficacy and Safety of the mRNA-1273 SARS-CoV-2 Vaccine. *N Engl J Med* **384**, 403-416, https://doi.org/10.1056/NEJMoa2035389 (2021).
27. Corbett, K. S. et al. Evaluation of the mRNA-1273 Vaccine against SARS-CoV-2 in Nonhuman Primates. *N Engl J Med* **383**, 1544-1555, https://doi.org/10.1056/NEJMoa2024671 (2020).
28. Vogel, A. B. et al. BNT162b vaccines protect rhesus macaques from SARS-CoV-2. *Nature* **592**, 283-289, https://doi.org/10.1038/s41586-021-03275-y (2021).
29. Liu, C. et al. Reduced neutralization of SARS-CoV-2 B.1.617 by vaccine and convalescent serum. *Cell*, https://doi.org/10.1016/j.cell.2021.06.020 (2021).
30. Haas, E. J. et al. Impact and effectiveness of mRNA BNT162b2 vaccine against SARS-CoV-2 infections and COVID-19 cases, hospitalisations, and deaths following a nationwide vaccination campaign in Israel: an observational study using national surveillance data. *Lancet* **397**, 1819-1829, https://doi.org/10.1016/S0140-6736(21)00947-8 (2021).
31. Wu, K. et al. Serum Neutralizing Activity Elicited by mRNA-1273 Vaccine. *N Engl J Med* **384**, 1468-1470, https://doi.org/10.1056/NEJMc2102179 (2021).
32. Wibmer, C. K. et al. SARS-CoV-2 501Y.V2 escapes neutralization by South African COVID-19 donor plasma. *Nat Med* **27**, 622-625, https://doi.org/10.1038/s41591-021-01285-x (2021).
33. Wall, E. C. et al. Neutralising antibody activity against SARS-CoV-2 VOCs B.1.617.2 and B.1.351 by BNT162b2 vaccination. *Lancet* **397**, 2331-2333, https://doi.org/10.1016/S0140-6736(21)01290-3 (2021).
34. Philipp, M. & Santibanez, G. Preference of respiratory phases to perform reaction time tasks. *Act Nerv Super (Praha)* **30**, 153-155 (1988).
35. Feng, S. et al. Correlates of protection against symptomatic and asymptomatic SARS-CoV-2 infection. *medRxiv*, 2021.2006.2021.21258528, https://doi.org/10.1101/2021.06.21.21258528 (2021).
36. Lafon, E. et al. Potent SARS-CoV-2-Specific T Cell Immunity and Low Anaphylatoxin Levels Correlate With Mild Disease Progression in COVID-19 Patients. *Front Immunol* **12**, 684014, https://doi.org/10.3389/fimmu.2021.684014 (2021).
37. Schmidt, M. E. & Varga, S. M. The CD8 T Cell Response to Respiratory Virus Infections. *Front Immunol* **9**, 678, https://doi.org/10.3389/fimmu.2018.00678 (2018).
38. Abayasingam, A. et al. Long-term persistence of RBD(+) memory B cells encoding neutralizing antibodies in SARS-CoV-2 infection. *Cell Rep Med* **2**, 100228, https://doi.org/10.1016/j.xcrm.2021.100228 (2021).
39. Dan, J. M. et al. Immunological memory to SARS-CoV-2 assessed for up to 8 months after infection. *Science* **371**, https://doi.org/10.1126/science.abf4063 (2021).
40. Graham, B. S. Rapid COVID-19 vaccine development. *Science* **368**, 945-946, https://doi.org/10.1126/science.abb8923 (2020).

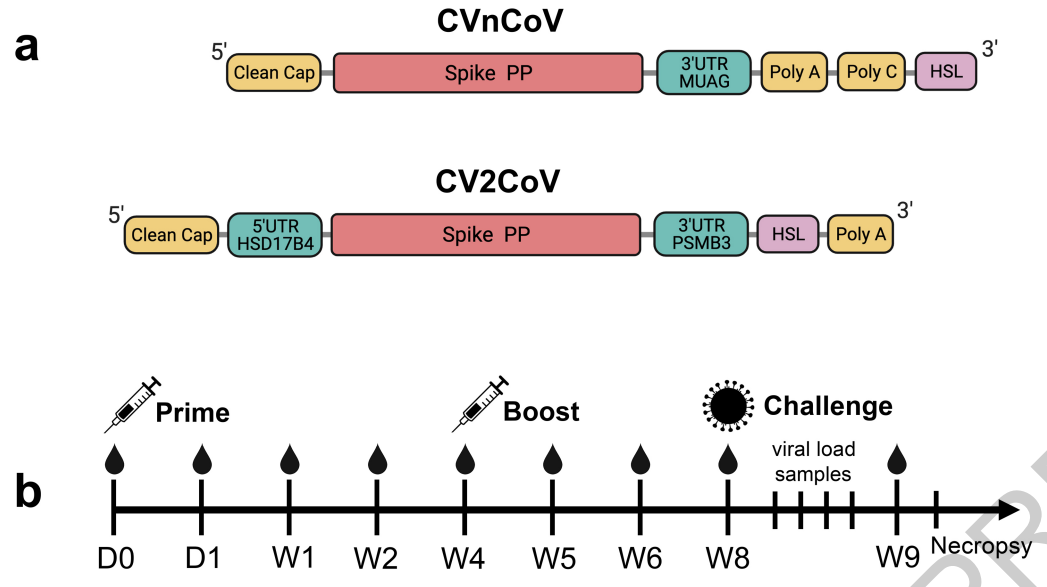

Groups (N=6)	Vaccines	Antigen	Dose	Route
I	Sham	Sham	Sham	Sham
II	CVnCoV	Full length Spike (K986P, V987P)	12μg	I.M.
III	CV2CoV	Full length Spike (K986P, V987P)	12μg	I.M.

Fig. 1 | Vaccine design and study schema. (a) Design of CVnCOV and CV2CoV mRNA vaccine candidates. Both vaccines are based on CureVac's RNActive® platform and encode for SARS-COV-2 Spike protein with di-proline mutations. The vaccines differ in their unique non-coding regions as shown. (b) NHP vaccine study schema. Cynomolgus macaques were immunized on day 0 with CVnCoV (N=6) or CV2CoV (N=6) mRNA vaccines or were designated as sham (N=6). The animals were boosted at week 4 and challenged at week 8. Samples were collected weekly post immunization and on days 0, 1, 2, 4, 7 and 10 post challenge for immunological and virological assays. I.M. = intramuscular.

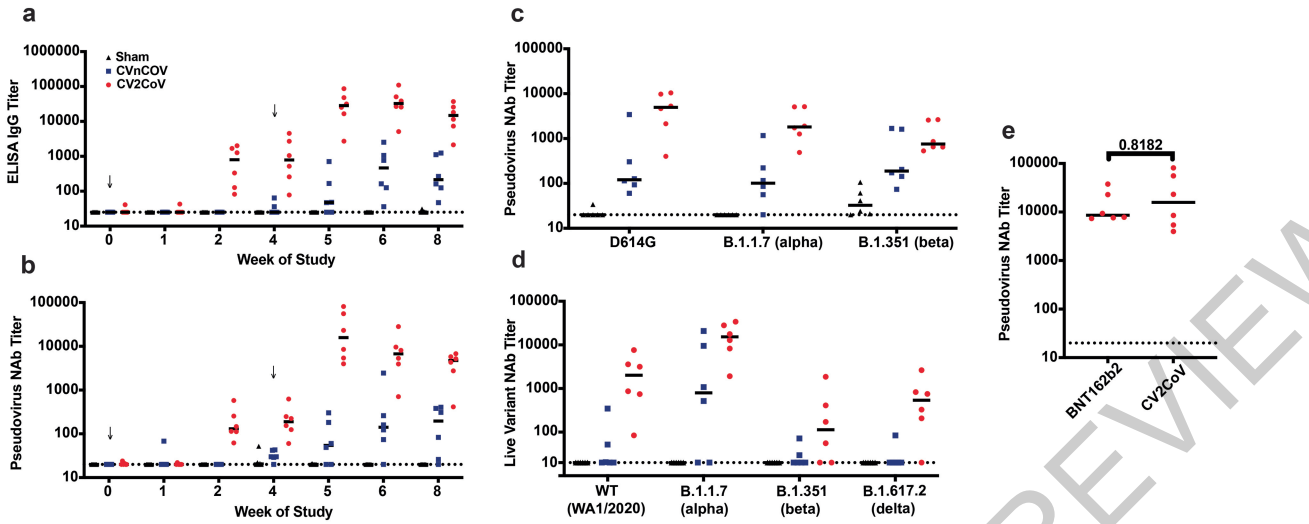

Fig. 2 | CV2CoV elicits high levels of binding and neutralizing antibody responses in macaques. Animals (6/group) were vaccinated twice with 12µg of CVnCoV or CV2CoV on d0 and d28 or remained untreated as negative controls (sham). (a) Titers of RBD binding antibodies and (b) pseudovirus neutralizing antibodies against ancestral SARS-CoV-2 strain were evaluated at different time points post first (week 0, 1, 2 and 4) and second (week 5, 6 and 8) vaccinations. (c) Sera isolated on d42 (week 6) were analyzed for (c) pseudovirus and (d) live variant neutralizing antibody titers against virus containing the D614G mutation and the B.1.1.7 (Alpha) and B.1.351 (Beta) variants. (e) Sera isolated from NHPs immunized with 12µg of CVnCoV or 30µg of BNT162b2 on d35 (week 5) post boost were analyzed for pseudovirus neutralizing antibody titers against the ancestral WA/2020 (WT) strain. Each dot represents an individual animal, bars depict the median and the dotted line shows limit of detection.

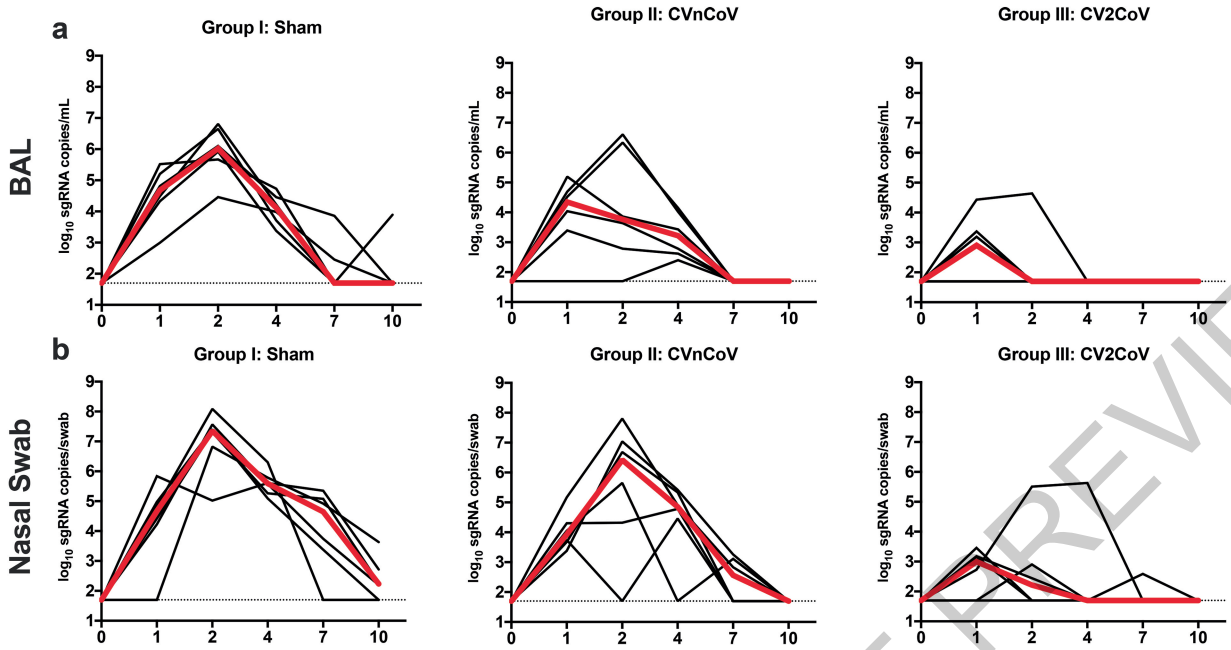

Fig. 3 | Protective efficacy of CV2CoV. Negative control (sham) or animals (6/group) vaccinated on d0 and d28 with 12µg of CVnCoV or CV2CoV were challenged with 1.0×10^5 $TCID_{50}$ SARS-CoV-2 (USA-WA1/2020) via the intranasal (IN) and intratracheal (IT) routes. BAL (a) and nasal swab samples (b) collected on days 1, 2, 4, 7 and 10 post-challenge were analyzed for levels of replicating virus by RT-PCR specific for subgenomic mRNA (sgRNA). Thin black lines represent an individual animal, thick red lines depict the median and the dotted line shows limit of detection. BAL = bronchoalveolar lavage.

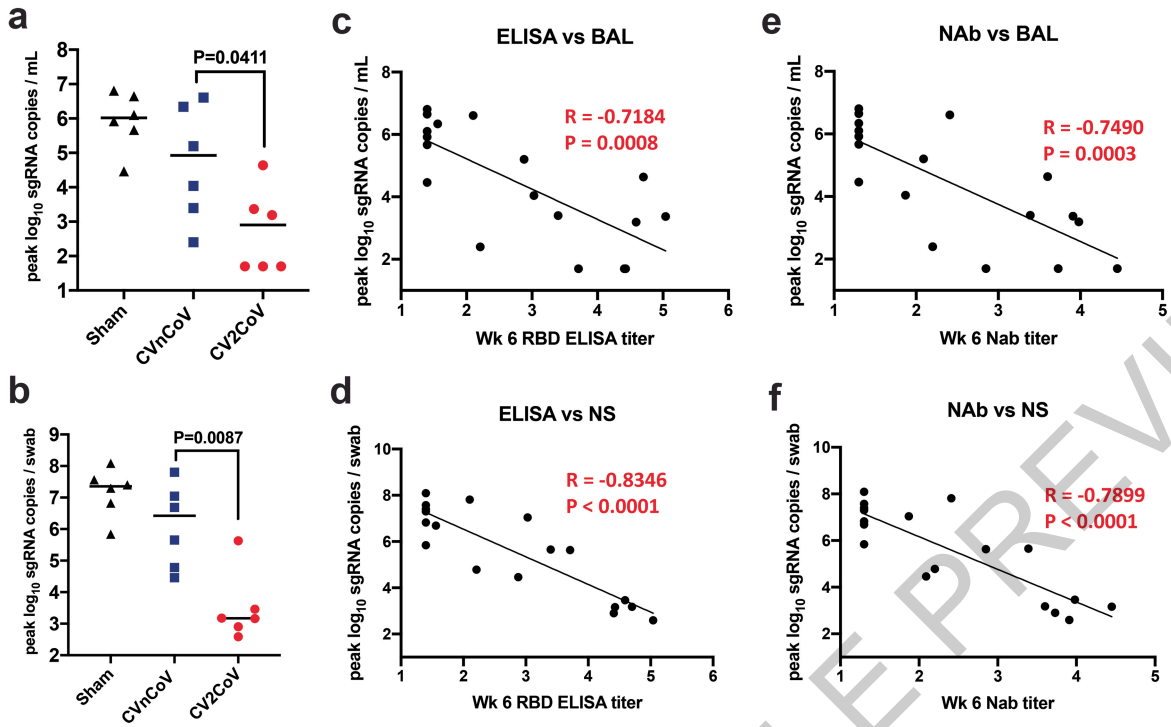

Fig. 4 | Titers of binding and neutralizing antibody titers elicited upon CVnCoV and CV2CoV vaccination (6/group) correlate with protection against SARS-CoV-2. Summary of peak viral loads following SARS-CoV-2 challenge in BAL and nasal swab. Animals were challenged with $1.0x10^5$ $TCID_{50}$ SARS-CoV-2 derived from USA-WA1/2020 (NR-52281; BEI Resources) (a, b); antibody correlates of protection for binding antibodies (c, d) and neutralizing antibodies (e, f). Statistical analysis was performed using two-tailed nonparametric Mann-Whitney test. Correlations was analyzed by two-sided Spearman rank-correlation test. NAbs = neutralizing antibodies, BAL = bronchoalveolar lavage NS = nasal swab.

Methods

mRNA vaccines

The two mRNA vaccines, CVnCoV and CV2CoV, are based on CureVac's RNActive® platform (claimed and described in e.g. WO2002098443 and WO2012019780) and do not include chemically modified nucleosides. They are comprised of a 5′ cap1 structure, a GC-enriched open reading frame (ORF), 3′ UTR and a vector-encoded poly-A stretch. CVnCoV contains a cleanCap (Trilink), parts of the 3′ UTR of the Homo sapiens alpha haemoglobin gene as 3′ UTR, followed by a poly-A (64) stretch, a polyC (30) stretch and a histone stem loop[23,24]. CV2CoV has previously been described to contain a cleanCap followed by 5′ UTR from the human hydroxysteroid 17-beta dehydrogenase 4 gene (HSD17B4) and a 3′ UTR from human proteasome 20S subunit beta 3 gene (PSMB3), followed by a histone stem loop and a poly-A (100) stretch[3]. Both constructs were encapsulated in lipid nanoparticles (LNP) by Acuitas Therapeutics (Vancouver, Canada) (CV2CoV) or Polymun Scientific Immunbiologische Forschung GmbH (Klosterneuburg, Austria) (CVnCoV). LNPs are composed of ionizable amino lipid, phospholipid, cholesterol, and a PEGylated lipid; compositions for CVnCoV and CV2CoV are identical. Both mRNAs encode for SARS-CoV-2 full length spike protein containing stabilizing K986P and V987P mutations (NCBI Reference Sequence NC_045512.2).

Animals and study design

18 cynomolgus macaques of both sexes between the ages of 3-20 were randomly assigned to three groups. Animals received either CVnCoV (N=6) or CV2CoV (N=6) mRNA vaccines or were designated as sham controls (N=6). The mRNA vaccines were administered at a 12 µg dose, intramuscularly, in the left quadriceps on day 0. Boost immunizations were similarly administered at week 4. At week 8, all animals were challenged with $1.0x10^5$ $TCID_{50}$ SARS-CoV-2 derived from USA-WA1/2020 (NR-52281; BEI Resources)[17]. Challenge virus was administered as 1 ml by the intranasal (IN) route (0.5 ml in each nare) and 1 ml by the intratracheal (IT) route. All animals were sacrificed 10 days post challenge. Immunologic and virologic assays were performed blinded. All animals were housed at Bioqual, Inc. (Rockville, MD). All animal studies were conducted in compliance with all relevant local, state, and federal regulations and were approved by the Bioqual Institutional Animal Care and Use Committee (IACUC).

Cytokine analyses

Serum levels of 19 analytes that have been associated with immune response to viral infection were tested using U-PLEX Viral Combo 1 (NHP) kit (K15069L-1) from Meso Scale Discovery (MSD, Rockville, MD). The 19 analytes and their detection limits (LLODs) are G-CSF (1.5 pg/mL), GM-CSF (0.12 pg/mL), IFN-α2a (1.7 pg/mL), IFN-γ (1.7 pg/mL), IL-1RA (1.7 pg/mL), IL-1β (0.15 pg/mL), IL-4 (0.06 pg/mL), IL-5 (0.24 pg/mL), IL-6 (0.33 pg/mL), IL-7 (1.5 pg/mL) and IL-8 (0.15 pg/mL), IL-9 (0.14 pg/mL), IL-10 (0.14 pg/mL), IL-12p70 (0.54 pg/mL), IP-10 (0.49 pg/mL), MCP-1 (0.74 pg/mL), MIP-1α (7.7 pg/mL), TNF-α (0.54 pg/mL) and VEGF-A (2.0pg/mL). All serum samples were assayed in duplicate. Assay was done by the Metabolism and Mitochondrial Research Core (Beth Israel Deaconess Medical Center, Boston, MA) following manufacture's instruction. The assay plates were read by MESO QUICKPLEX SQ 120 instrument and data were analyzed by DISCOVERY WORKBENCH® 4.0 software.

Enzyme-linked immunosorbent assay (ELISA)

RBD-specific binding antibodies were assessed by ELISA as described[16,17]. Briefly, 96-well plates were coated with 1µg/ml SARS-CoV-2 RBD protein (40592-VNAH, SinoBiological) in 1X DPBS and incubated at 4 °C overnight. After incubation, plates were washed once with wash buffer (0.05% Tween 20 in 1 X DPBS) and blocked with 350 µL casein block/well for 2–3 h at room temperature. After incubation, block solution was discarded, and plates were blotted dry. Serial dilutions of heat-inactivated serum diluted in casein block were added to wells and plates were incubated for 1 h at room temperature. Next, the plates were washed three times and incubated for 1 h with a 1:1000 dilution of anti-macaque IgG HRP (NIH NHP Reagent Program) at room temperature in the dark. Plates were then washed three more times, and 100 µL of SeraCare KPL TMB SureBlue Start solution was added to each well; plate development was halted by the addition of 100 µL SeraCare KPL TMB Stop solution per well. The absorbance at 450nm was recorded using a VersaMax or Omega microplate reader. ELISA endpoint titers were defined as the highest reciprocal serum dilution that yielded an absorbance > 0.2. Log10 endpoint titers are reported. Immunologic assays were performed blinded.

Pseudovirus neutralization assay

The SARS-CoV-2 pseudoviruses expressing a luciferase reporter gene were generated as described previously[15]. Briefly, the packaging plasmid psPAX2 (AIDS Resource and Reagent Program), luciferase reporter plasmid pLenti-CMV Puro-Luc (Addgene), and spike protein expressing pcDNA3.1-SARS CoV-2 SΔCT of variants were co-transfected into HEK293T cells by lipofectamine 2000 (ThermoFisher). Pseudoviruses of SARS-CoV-2 variants were generated by using WA1/2020 strain (Wuhan/WIV04/2019, GISAID accession ID: EPI_ISL_402124), D614G mutation, B.1.1.7 variant (GISAID accession ID: EPI_ISL_601443), B.1.351 variant (GISAID accession ID: EPI_ISL_712096), C37 variant (GenBank ID: QRX62290), B.1.671.1 variant (GISAID accession ID: EPI_ISL_1384866) and B.1.617.2 variant (GISAID accession ID: EPI_ISL_2020950). The supernatants containing the pseudotype viruses were collected 48 h post-transfection, which were purified by centrifugation and filtration with 0.45 µm filter. To determine the neutralization activity of the plasma or serum samples from participants, HEK293T-hACE2 cells were seeded in 96-well tissue culture plates at a density of 1.75×10^4 cells/well overnight. Three-fold serial dilutions of heat inactivated serum or plasma samples were prepared and mixed with 50 µL of pseudovirus. The mixture was incubated at 37ºC for 1 h before adding to HEK293T-hACE2 cells. 48 h after infection, cells were lysed in Steady-Glo Luciferase Assay (Promega) according to the manufacturer's instructions. SARS-CoV-2 neutralization titers were defined as the sample dilution at which a 50% reduction in relative light unit (RLU) was observed relative to the average of the virus control wells.

Live virus neutralization assay

Full-length SARS-CoV-2 WA1/2020, B.1.1.7, B.1.351 and B.1.617.2, viruses were designed to express nanoluciferase (nLuc) and were recovered via reverse genetics[18]. One day before the assay, Vero E6 USAMRID cells were plated at 20,000 cells per well in clear-bottom black-walled plates. Cells were inspected to ensure confluency on the day of assay. Serum samples were tested at a starting dilution of 1:20 and were serially diluted threefold up to nine dilution spots. Serially diluted serum samples were mixed in equal volume with diluted virus. Antibody–virus and virus-only mixtures were then incubated at 37 °C with 5% CO2 for 1 h. After incubation, serially diluted sera and virus-only controls were added in duplicate to the cells at 75 plaque-forming units at 37 °C with 5% CO2. Twenty-four hours later, the cells were lysed, and luciferase activity was measured via Nano-Glo Luciferase Assay System (Promega) according to the manufacturer specifications. Luminescence was measured by a Spectramax M3 plate reader (Molecular Devices). Virus neutralization titres were defined as the sample dilution at which a 50% reduction in RLU was observed relative to the average of the virus control wells.

B cell immunophenotyping

Fresh PBMCs were stained with Aqua live/dead dye (Invitrogen) for 20 min, washed with 2% FBS/DPBS buffer, and suspended in 2% FBS/DPBS buffer with Fc Block (BD) for 10 min, followed by staining with monoclonal antibodies against CD45 (clone D058-1283, BUV805), CD3 (clone SP34.2, APC-Cy7), CD7 (clone M-T701, Alexa700), CD123 (clone

6H6, Alexa700), CD11c (clone 3.9, Alexa700), CD20 (clone 2H7, PE-Cy5), IgA (goat polyclonal antibodies, APC), IgG (clone G18-145, BUV737), IgM (clone G20-127, BUV396), IgD (goat polyclonal antibodies, PE), CD80 (clone L307.4, BV786), CD95 (clone DX2, BV711), CD27 (clone M-T271, BUV563), CD21 (clone B-ly4, BV605), CD14 (clone M5E2, BV570) and CD138 (clone DL-101, PE-CF594). Cells were also stained with SARS-CoV-2 antigens including biotinylated SARS-CoV-2 RBD protein (Sino Biological) and full-length SARS-CoV-2 Spike protein (Sino Biological) labeled with FITC and DyLight 405 (DyLight® 405 Conjugation Kit, FITC Conjugation Kit, Abcam), at 4 °C for 30 min. After staining, cells were washed twice with 2% FBS/DPBS buffer, followed by incubation with BV650 streptavidin (BD Pharmingen) for 10min, then washed twice with 2% FBS/DPBS buffer. After staining, cells were washed and fixed by 2% paraformaldehyde. All data were acquired on a BD FACSymphony flow cytometer. Subsequent analyses were performed using FlowJo software (Treestar, v.9.9.6). Immunologic assays were performed blinded.

IFN-γ enzyme-linked immunospot (ELISPOT) assay

ELISPOT plates were coated with mouse anti-human IFN-γ monoclonal antibody from BD Pharmingen at a concentration of 5 µg/well overnight at 4 °C. Plates were washed with DPBS containing 0.25% Tween 20, and blocked with R10 media (RPMI with 11% FBS and 1.1% penicillin-streptomycin) for 1 h at 37 °C. The Spike 1 and Spike 2 peptide pools (JPT Peptide Technologies, custom made) used in the assay contain 15 amino acid peptides overlapping by 11 amino acids that span the protein sequence and reflect the N- and C- terminal halves of the protein, respectively. Spike 1 and Spike 2 peptide pools were prepared at a concentration of 2 µg/well, and 200,000 cells/well were added. The peptides and cells were incubated for 18–24 h at 37 °C. All steps following this incubation were performed at room temperature. The plates were washed with ELISPOT wash buffer and incubated for 2 h with rabbit polyclonal anti-human IFN-γ Biotin from U-Cytech (1 µg/mL). The plates are washed a second time and incubated for 2 h with Streptavidin-alkaline phosphatase antibody from Southern Biotechnology (1 µg/mL). The final wash was followed by the addition of nitro-blue tetrazolium chloride/5-bromo-4-chloro 3 'indolyl phosphate p-toludine salt (NBT/BCIP chromagen) substrate solution (Thermo Scientific) for 7 min. The chromogen was discarded and the plates were washed with water and dried in a dim place for 24 h. Plates were scanned and counted on a Cellular Technologies Limited Immunospot Analyzer.

IL-4 ELISPOT assay

Precoated monoclonal antibody IL-4 ELISPOT plates (Mabtech) were washed and blocked. The assay was then performed as described above except the development time with NBT/BCIP chromagen substrate solution was 12 min.

Subgenomic RT-PCR assay

SARS-CoV-2 E gene subgenomic RNA (sgRNA) was assessed by RT-PCR using primers and probes as previously described[15,17]. A standard was generated by first synthesizing a gene fragment of the subgenomic E gene. The gene fragment was subsequently cloned into a pcDNA3.1+ expression plasmid using restriction site cloning (Integrated DNA Technologies). The insert was in vitro transcribed to RNA using the AmpliCap-Max T7 High Yield Message Maker Kit (CellScript). Log dilutions of the standard were prepared for RT-PCR assays ranging from $1x10^{10}$ copies to $1x10^{-1}$ copies. Viral loads were quantified from bronchoalveolar lavage (BAL) fluid and nasal swabs (NS). RNA extraction was performed on a QIAcube HT using the IndiSpin QIAcube HT Pathogen Kit according to manufacturer's specifications (Qiagen). The standard dilutions and extracted RNA samples were reverse transcribed using SuperScript VILO Master Mix (Invitrogen) following the cycling conditions described by the manufacturer. A Taqman custom gene expression assay (Thermo Fisher Scientific) was designed using the sequences targeting the E gene sgRNA. The sequences for the custom assay were as follows, forward primer, sgLeadCoV2.Fwd: CGATCTCTTGTAGATCTGTTCTC, E_Sarbeco_R: ATATTGCAGCAGTACGCACACA, E_Sarbeco_P1 (probe): VIC-ACACTAGCCATCCTTACTGCGCTTCG-MGBNFQ. Reactions were carried out in duplicate for samples and standards on the QuantStudio 6 and 7 Flex Real-Time PCR Systems (Applied Biosystems) with the thermal cycling conditions: initial denaturation at 95 °C for 20 seconds, then 45 cycles of 95 °C for 1 second and 60 °C for 20 seconds. Standard curves were used to calculate subgenomic RNA copies per ml or per swab. The quantitative assay sensitivity was determined as 50 copies per ml or per swab.

$TCID_{50}$ assay

Vero TMPRSS2 cells (obtained from A. Creanga) were plated at 25,000 cells per well in DMEM with 10% FBS and gentamicin, and the cultures were incubated at 37 °C, 5.0% CO_2. Medium was aspirated and replaced with 180 µl of DMEM with 2% FBS and gentamicin. Serial dilution of samples as well as positive (virus stock of known infectious titre) and negative (medium only) controls were included in each assay. The plates are incubated at 37 °C, 5.0% CO_2 for 4 days. Cell monolayers were visually inspected for cytopathic effect. The $TCID_{50}$ was calculated using the Read–Muench formula.

Histopathology

At time of fixation, lungs were suffused with 10% formalin to expand the alveoli. All tissues were fixed in 10% formalin and blocks sectioned at 5 µm. Slides were baked for 30-60 min at 65 degrees, deparaffinized in xylene, rehydrated through a series of graded ethanol to distilled water, then stained with hematoxylin and eosin (H&E). Blinded histopathological evaluation was performed by a board-certified veterinary pathologist (AJM).

Statistical analyses

Statistical analyses were performed using GraphPad Prism (version 9.0) software (GraphPad Software) and comparison between groups was performed using a two-tailed nonparametric Mann-Whitney U t test. P-values of less than 0.05 were considered significant. Correlations were assessed by two-sided Spearman rank-correlation tests.

Reporting summary

Further information on research design is available in the Nature Research Reporting Summary linked to this paper.

Data availability

All data are available in the manuscript and the supplementary material. Source data are provided with this paper.

Acknowledgements We thank Sarah Gardner, Gabriella Kennedy, and Rachael Edmonston for their generous assistance. We thank Domenico Maione and Marie-Thérèse Martin for critically reading the manuscript. This work was supported by CureVac AG and the German Federal Ministry of Education and Research (BMBF; 01KI20703), the National Institutes of Health (CA260476), the Massachusetts Consortium on Pathogen Readiness, and Ragon Institute of MGH, MIT, and Harvard. Development of CV2CoV is carried out in a collaboration of CureVac AG and GSK.

Author contributions S.R., B.P., S.O.M., N.R. and D.H.B. designed the study. M.S.G., J.Y., A.C., N. M., X. H., J. L., K. M., A. M., D.R.M., R.S.B, A.C.M.B., T.G., D.H., S.P., D.S., O.S., and J.B. performed immunologic and virologic assays. X.L. and A.C.C. performed cytokine analysis. L.P., D.V., Z.F., J.Y., J.M., R.B., A.C., E.T., H.A. and M.L. led the clinical care of the animals. M.S.G. and D.H.B. wrote the paper with all coauthors.

Competing interests S.R., B.P., N.R., and S.O.M. are employees of CureVac AG, Tübingen, Germany, a publicly listed company developing mRNA-based vaccines and immunotherapeutics. Authors may hold shares in the company. S.R. and B.P. and N.R. are inventors on several patents on mRNA vaccination and use thereof. The other authors declare no competing interests.

Additional information
Supplementary information The online version contains supplementary material available at https://doi.org/10.1038/s41586-021-04231-6.
Correspondence and requests for materials should be addressed to Susanne Rauch or Dan H. Barouch.
Peer review information *Nature* thanks Wolfgang Baumgärtner and the other, anonymous, reviewer(s) for their contribution to the peer review of this work.

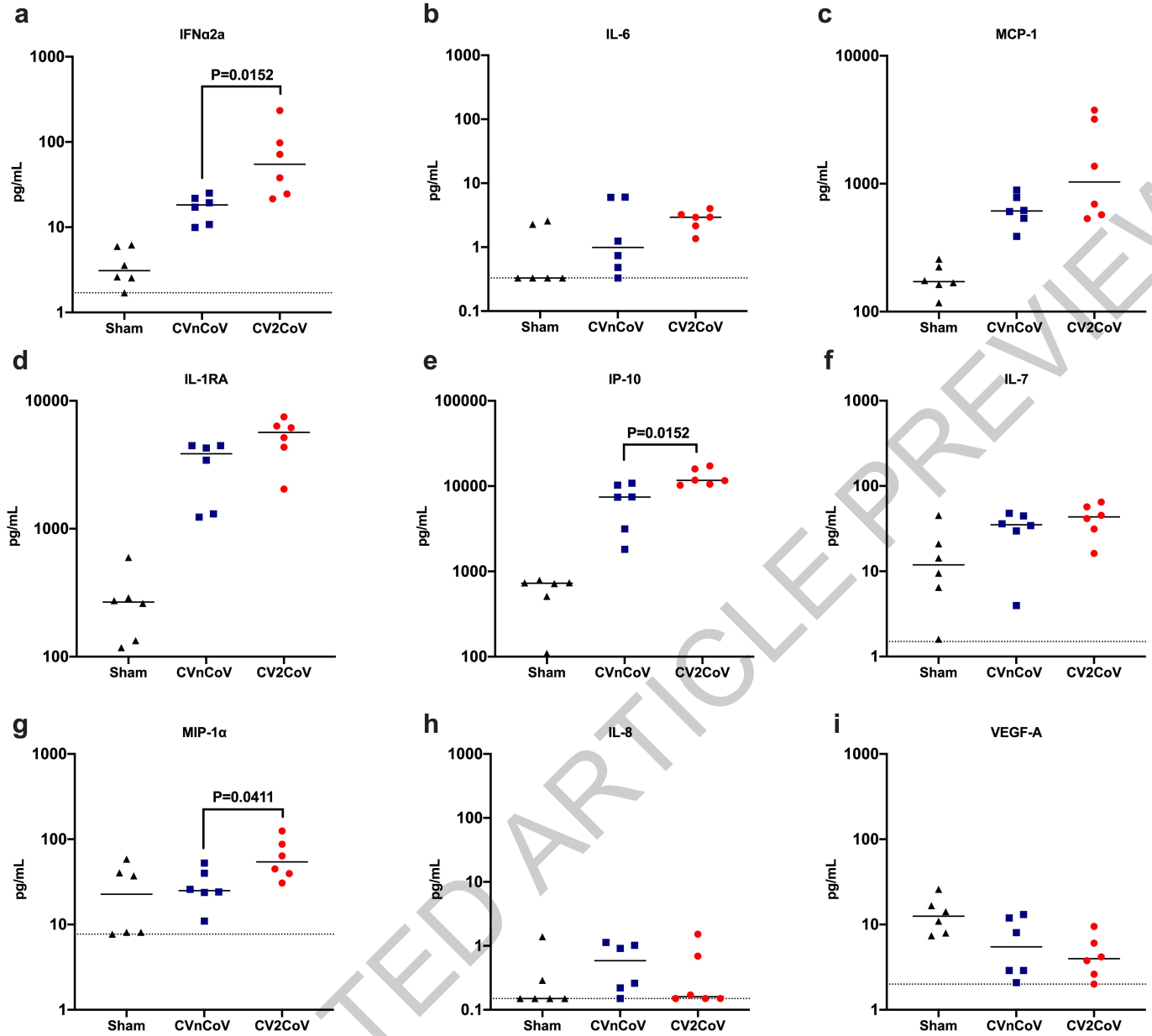

Extended Data Fig. 1 | Innate cytokine induction following mRNA immunization (6/group). Sera isolated 24h post first injection were analyzed for a panel of 19 cytokines associated with viral infection using a U-PLEX Viral Combo kit from Meso Scale Discovery. Changes in cytokine levels above the detection limits were detectable for 9 cytokines. Each dot represents an individual animal, bars depict the median and the dotted line shows limit of detection. Statistical analysis was performed using two-tailed nonparametric Mann-Whitney test.

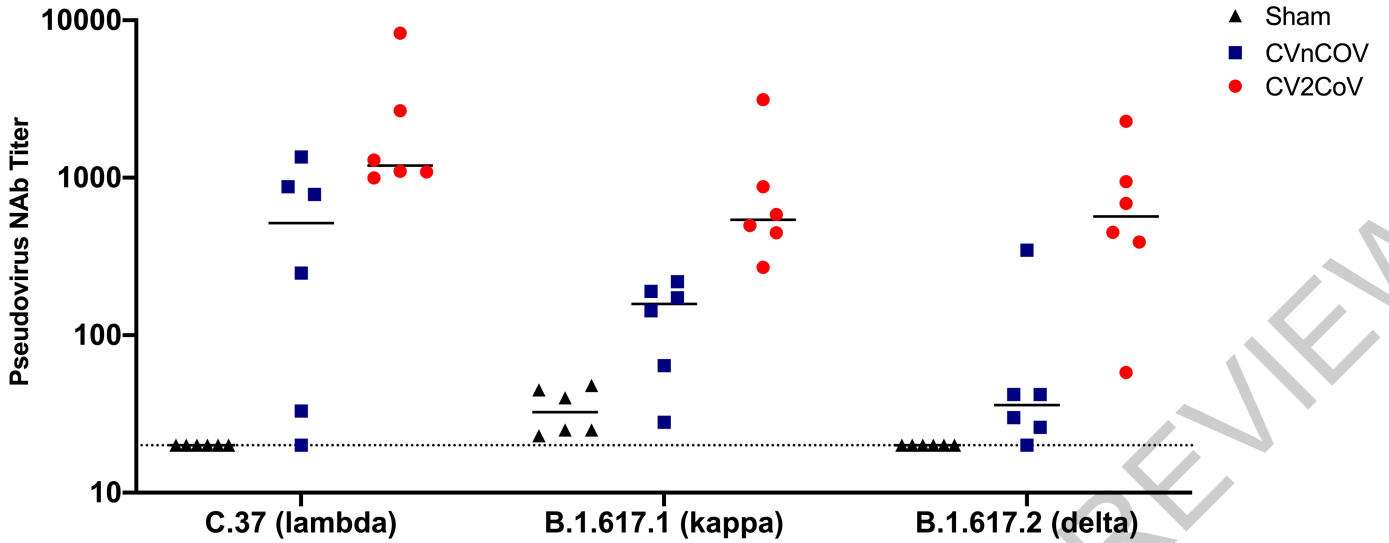

Extended Data Fig. 2 | Neutralizing antibody titers against variants. Animals (6/group) were vaccinated twice with 12µg of CVnCoV or CV2CoV on d0 and d28 or remained untreated as negative controls (sham). Sera isolated on d42 (week 6) were analyzed for pseudovirus neutralizing antibody titers against C.37 (Lambda), B.1.617.1 (Kappa) and B.1.617.2 (Delta) variants. Each dot represents an individual animal, bars depict the median and the dotted line shows limit of detection.

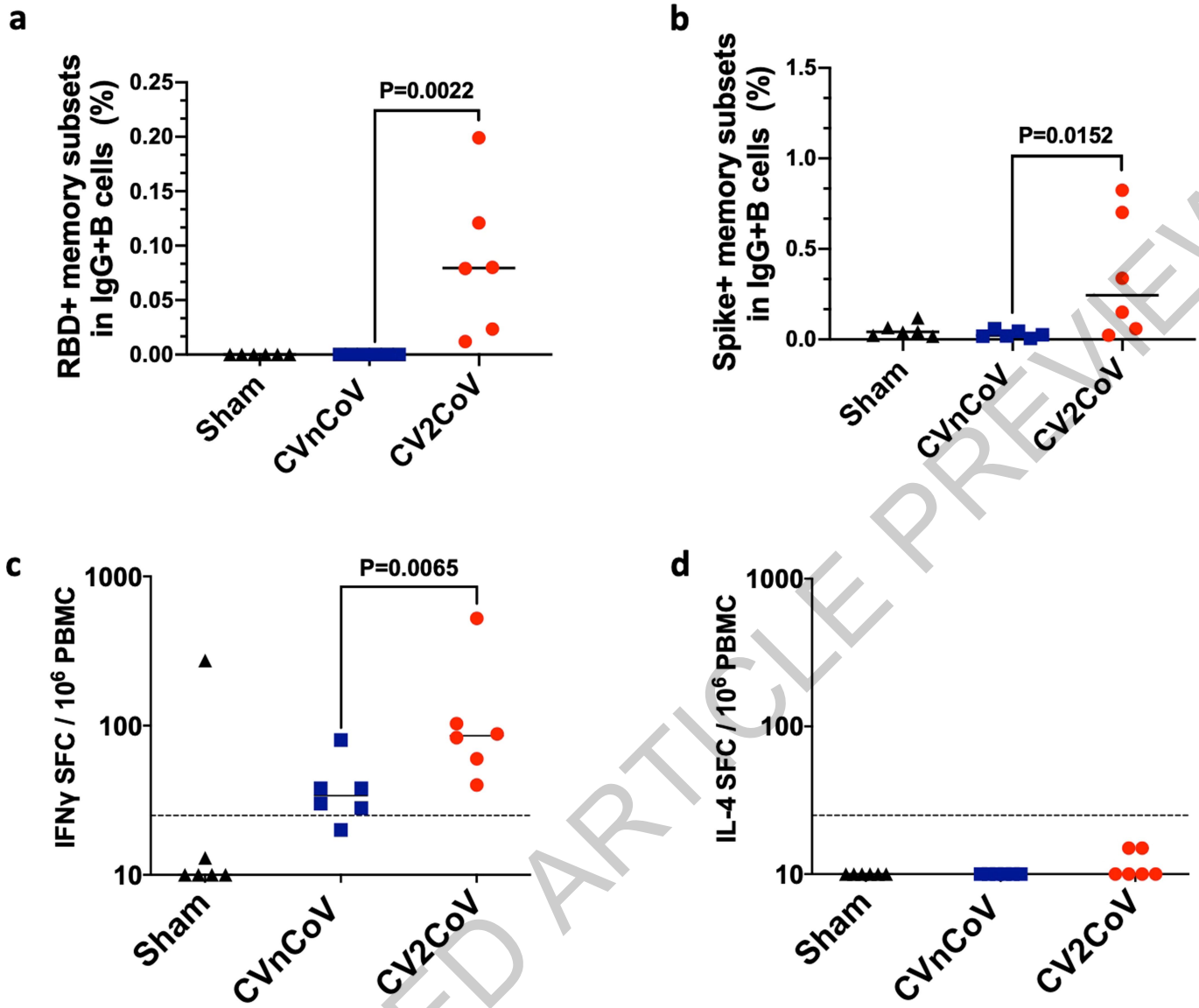

Extended Data Fig. 3 | Memory B and T cell immune responses day 42 following immunization. PBMCs from negative control (sham), CVnCoV or CV2CoV vaccinated animals (6/group) isolated on d42 of the experiment were stained for (a) RBD and (b) Spike-specific activated memory B cells and analyzed by high-parameter flow cytometry. IFNγ responses to pooled spike peptides were analyzed via ELISPOT (c). Each dot represents an individual animal, bars depict the median and the dotted line shows limit of detection. Statistical analysis was performed using two-tailed nonparametric Mann-Whitney test. PBMC = peripheral blood mononuclear cell; SFC = spot forming cells.

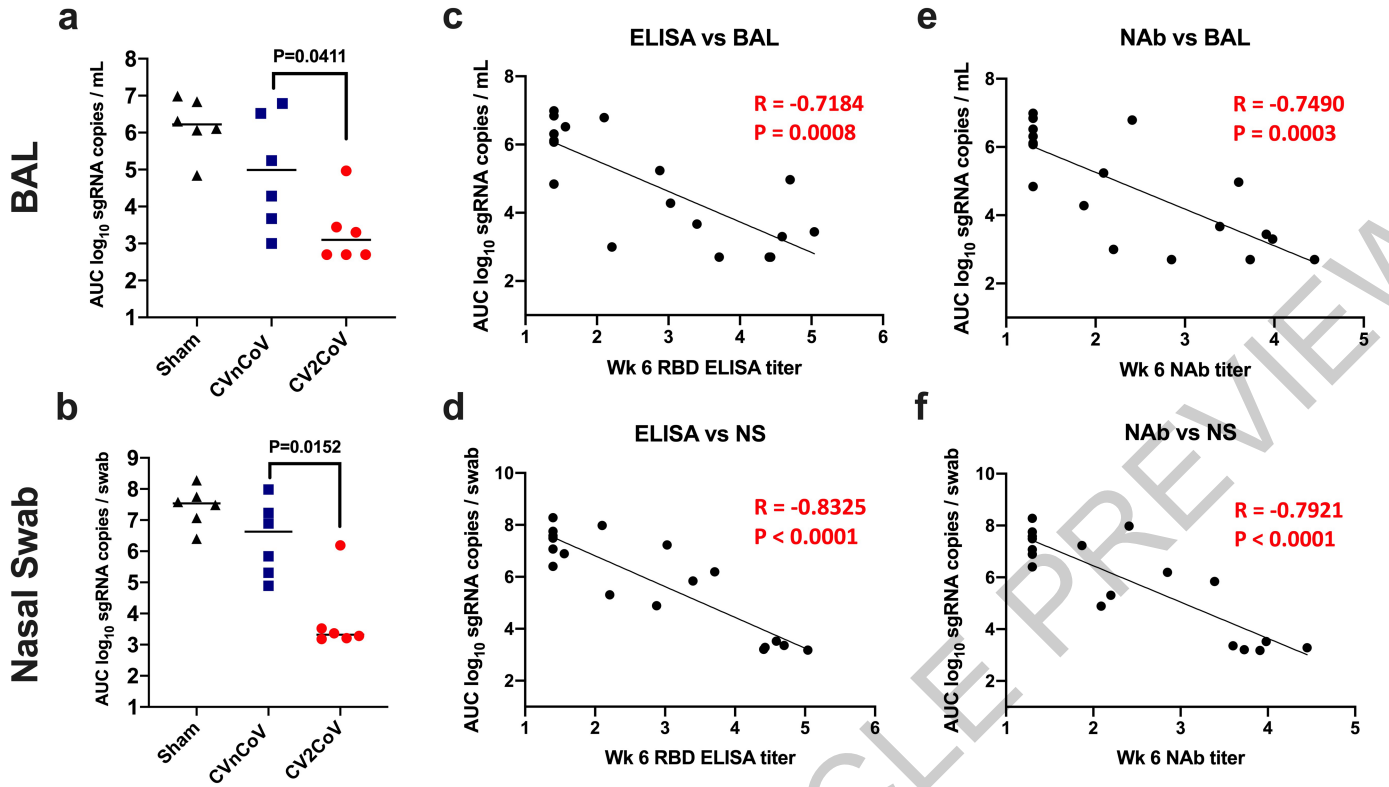

Extended Data Fig. 4 | Binding and neutralizing antibody titers correlate with protection against SARS-CoV-2. Summary of area under curve (AUC) viral load values following SARS-CoV-2 challenge in BAL and nasal swab samples (6/group) (a, b); antibody correlates of protection for binding antibodies (c, d) and neutralizing antibodies (e, f). Statistical analysis was performed using two-tailed nonparametric Mann-Whitney test. Correlations was analyzed by two-sided Spearman rank-correlation test. NAbs = neutralizing antibodies, BAL = bronchoalveolar lavage NS = nasal swab.

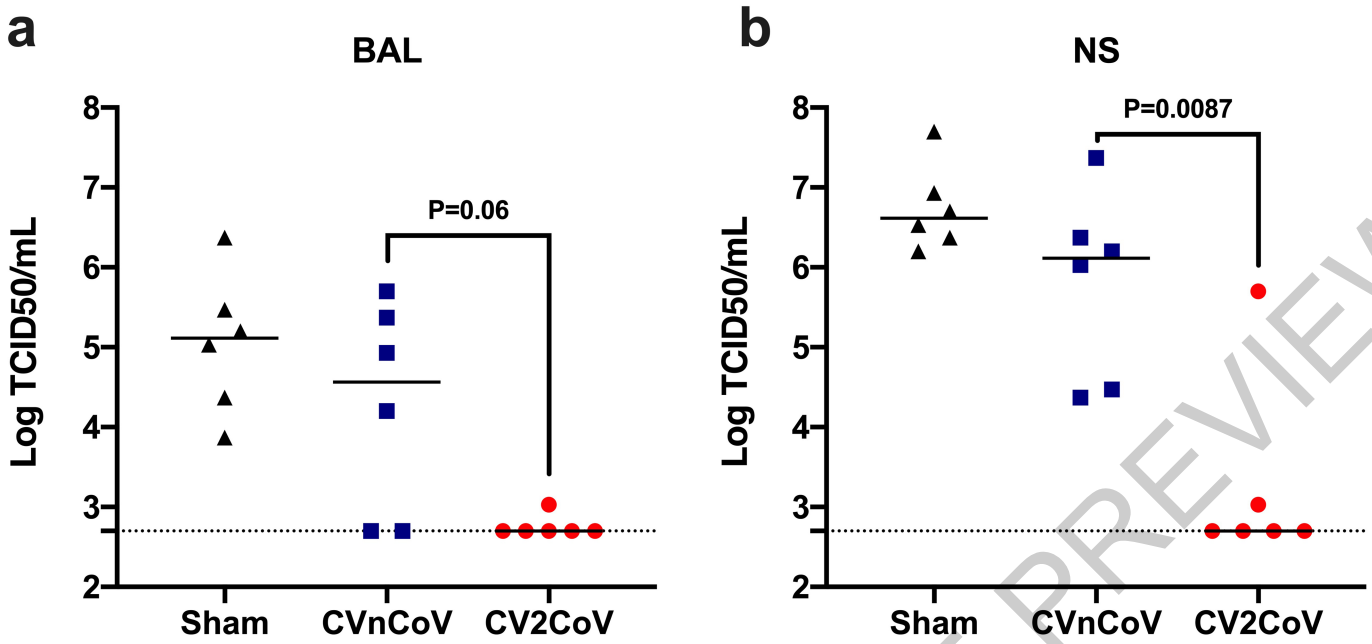

Extended Data Fig. 5 | Infectious virus titers after SARS-CoV-2 challenge (6/group). Infectious virus titers of BAL and nasal swab samples collected 2 days post challenge were analyzed by $TCID_{50}$ assays. Each dot represents an individual animal, bars depict the median and the dotted line shows limit of detection. Statistical analysis was performed using two-tailed nonparametric Mann-Whitney test.

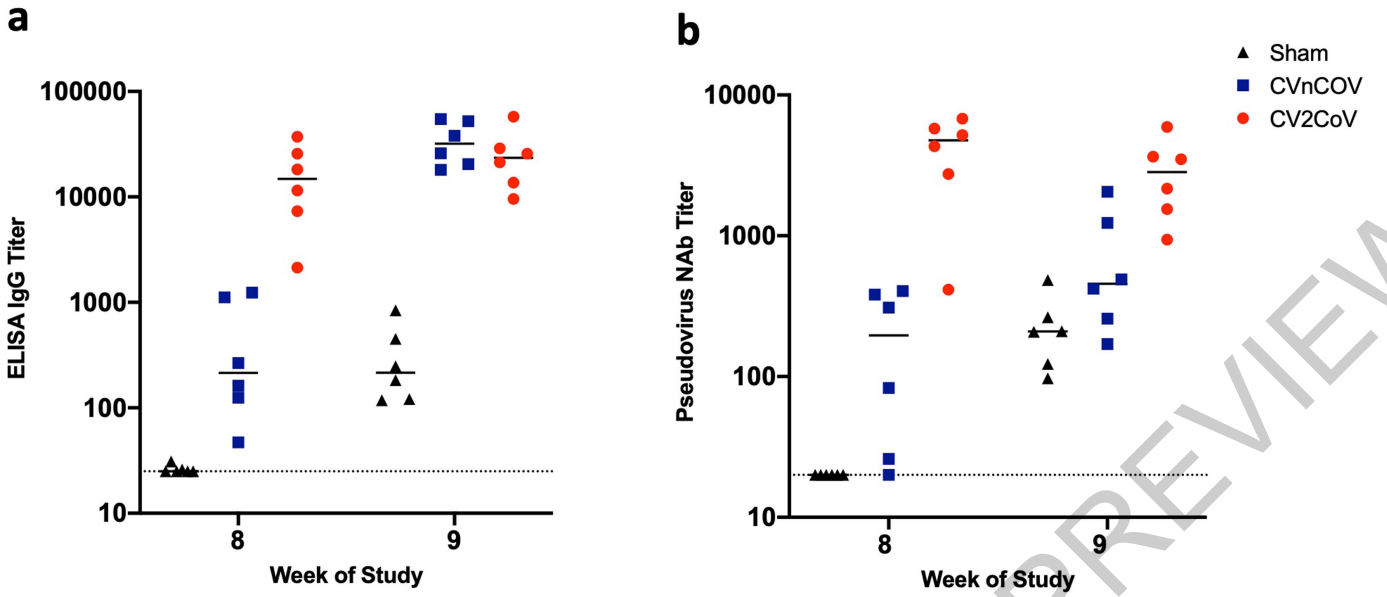

Extended Data Fig. 6 | Post-challenge binding and neutralizing antibody responses (6/group). Negative control (sham) or animals vaccinated on d0 and d28 of the experiment with 12µg of CVnCoV or CV2CoV as indicated were subjected to challenge infection using 1.0×10^5 $TCID_{50}$ SARS-CoV-2 via intranasal (IN) and intratracheal (IT) routes. (a) Titers of RBD binding antibodies and (b) pseudovirus neutralizing antibodies against ancestral SARS-CoV-2 strain were evaluated before (week 8) and a week after challenge infection (week 9). Each dot represents an individual animal, bars depict the median and the dotted line shows limit of detection. Statistical analysis was performed using two-tailed nonparametric Mann-Whitney test. NAbs= neutralizing antibodies.

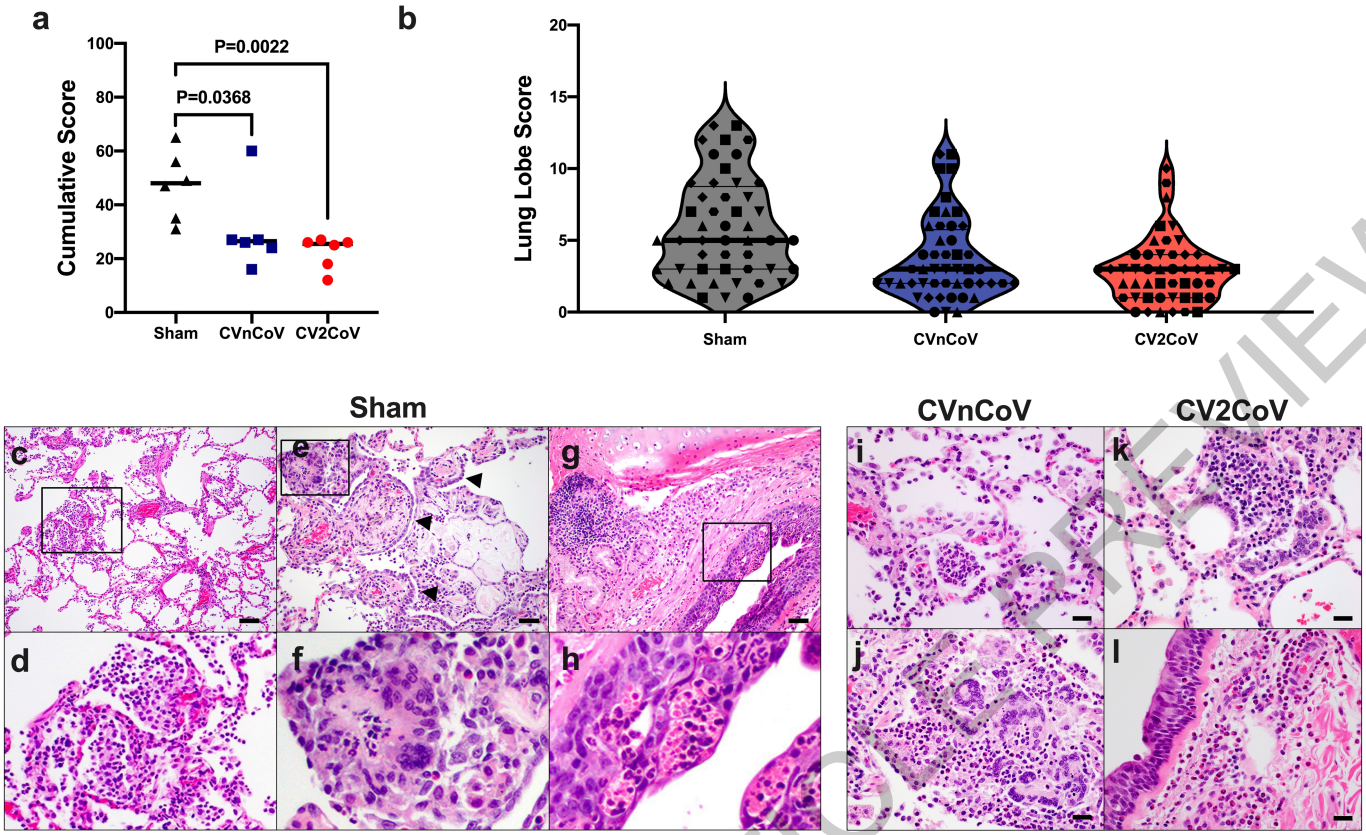

Extended Data Fig. 7 | CVnCoV and CV2CoV protect the lungs from pathological changes upon viral challenge (6/group). Eight lung lobes (4 sections from right and left, caudal to cranial) were assessed and scored (1-4) for each of the following lesions: 1) Interstitial inflammation and septal thickening 2) Eosinophilic interstitial infiltrate 3) Neutrophilic interstitial infiltrate 4) Hyaline membranes 5) Interstitial fibrosis 6) Alveolar infiltrate, macrophage 7) Alveolar/Bronchoalveolar infiltrate, neutrophils 8) Syncytial cells 9) Type II pneumocyte hyperplasia 10) Broncholar infiltrate, macrophage 11) Broncholar infiltrate, neutrophils 12) BALT hyperplasia 13) Bronchiolar/peribronchiolar inflammation 14) Perivascular, mononuclear infiltrates 15) Vessels, endothelialitis. Each feature assessed was assigned a score of 0= no significant findings; 1=minimal; 2= mild; 3=moderate; 4=marked/severe. (a) Cumulative scores per animal (b) Cumulative scores per lung lobe. Individual animals are represented by symbols. Representative histopathology from sham vaccinated (c-h), CnVCoV vaccinated (i, j), and Cv2CoV vaccinated (k, l) animals showing (c, d, inset) alveolar macrophage infiltrate, (e, f, inset) syncytial cells (arrowheads) and type II pneumocyte hyperplasia, inset (g, h, inset) bronchiolar epithelial necrosis with neutrophilic infiltrates (i) alveolar neutrophilic infiltrate and alveolar septal thickening (j) focal consolidation with inflammation composed of macrophages, neutrophils, and syncytial cells (k) focal pneumocyte hyperplasia, syncytial cells and inflammatory infiltrates (l) peribronchiolar inflammation. Statistical analysis was performed using two-tailed nonparametric Mann-Whitney test. Scale bars: 100 microns (c), 50 microns (e, g) 20 microns (i-l). BALT bronchus associated lymphoid tissue.

nature portfolio

Corresponding author(s): Dan Barouch 2021-08-13132

Last updated by author(s): Nov 7, 2021

Reporting Summary

Nature Portfolio wishes to improve the reproducibility of the work that we publish. This form provides structure for consistency and transparency in reporting. For further information on Nature Portfolio policies, see our Editorial Policies and the Editorial Policy Checklist.

Statistics

For all statistical analyses, confirm that the following items are present in the figure legend, table legend, main text, or Methods section.

n/a	Confirmed
☐	☒ The exact sample size (*n*) for each experimental group/condition, given as a discrete number and unit of measurement
☐	☒ A statement on whether measurements were taken from distinct samples or whether the same sample was measured repeatedly
☐	☒ The statistical test(s) used AND whether they are one- or two-sided *Only common tests should be described solely by name; describe more complex techniques in the Methods section.*
☐	☒ A description of all covariates tested
☐	☒ A description of any assumptions or corrections, such as tests of normality and adjustment for multiple comparisons
☐	☒ A full description of the statistical parameters including central tendency (e.g. means) or other basic estimates (e.g. regression coefficient) AND variation (e.g. standard deviation) or associated estimates of uncertainty (e.g. confidence intervals)
☐	☒ For null hypothesis testing, the test statistic (e.g. *F*, *t*, *r*) with confidence intervals, effect sizes, degrees of freedom and *P* value noted *Give P values as exact values whenever suitable.*
☒	☐ For Bayesian analysis, information on the choice of priors and Markov chain Monte Carlo settings
☒	☐ For hierarchical and complex designs, identification of the appropriate level for tests and full reporting of outcomes
☐	☒ Estimates of effect sizes (e.g. Cohen's *d*, Pearson's *r*), indicating how they were calculated

Our web collection on statistics for biologists contains articles on many of the points above.

Software and code

Policy information about availability of computer code

Data collection	Flow Jo Version 10.6.2 was used
Data analysis	Virologic and immunologic data analysis was performed using GraphPad Prism 9.0.0 (GraphPad Software). Specifically, cytokine data analysis was done using DISCOVERY WORKBENCH® 4.0 software.

For manuscripts utilizing custom algorithms or software that are central to the research but not yet described in published literature, software must be made available to editors and reviewers. We strongly encourage code deposition in a community repository (e.g. GitHub). See the Nature Portfolio guidelines for submitting code & software for further information.

Data

Policy information about availability of data

All manuscripts must include a data availability statement. This statement should provide the following information, where applicable:

- Accession codes, unique identifiers, or web links for publicly available datasets
- A description of any restrictions on data availability
- For clinical datasets or third party data, please ensure that the statement adheres to our policy

All data are available in the manuscript and the supplementary material.

Field-specific reporting

Please select the one below that is the best fit for your research. If you are not sure, read the appropriate sections before making your selection.

☒ Life sciences ☐ Behavioural & social sciences ☐ Ecological, evolutionary & environmental sciences

For a reference copy of the document with all sections, see nature.com/documents/nr-reporting-summary-flat.pdf

Life sciences study design

All studies must disclose on these points even when the disclosure is negative.

Sample size	Sample size includes N=18 animals (N=6 animals for each vaccine or sham control groups). Based on our previous experience with SARS-CoV-2 in cynomolgus as well as rhesus macaques, this sample size provides sufficient power to determine differences in protective efficacy of both vaccinated groups compared with the sham controls.
Data exclusions	No data were excluded.
Replication	Virologic and immunologic measures were performed in duplicate. Technical replicates were minimally different. Attempts in replication were succesful
Randomization	Animals were balanced for age and gender and otherwise randomly allocated to groups. All other sample randomization through out the study was random.
Blinding	All immunologic and virologic assays were performed blinded.

Reporting for specific materials, systems and methods

We require information from authors about some types of materials, experimental systems and methods used in many studies. Here, indicate whether each material, system or method listed is relevant to your study. If you are not sure if a list item applies to your research, read the appropriate section before selecting a response.

Materials & experimental systems

n/a	Involved in the study
☐	☒ Antibodies
☐	☒ Eukaryotic cell lines
☒	☐ Palaeontology and archaeology
☐	☒ Animals and other organisms
☒	☐ Human research participants
☒	☐ Clinical data
☒	☐ Dual use research of concern

Methods

n/a	Involved in the study
☒	☐ ChIP-seq
☒	☐ Flow cytometry
☒	☐ MRI-based neuroimaging

Antibodies

Antibodies used	For ELISA assay: anti-macaque IgG HRP (NIH NHP Reagent Program); for ELISPOT assay: mouse anti-human IFN-γ monoclonal antibody (BD Pharmingen), IL-4 capture monoclonal antibody (Mabtech), rabbit polyclonal anti-human IFN-γ Biotin (U-Cytech) and Streptavidin-alkaline phosphatase antibody (IFN-γ: Southern Biotechnology/IL-4 (Mabtech). For B cell ICS assay: monoclonal antibodies against CD45 (clone D058-1283, BUV805), CD3 (clone SP34.2 , APC-Cy7), CD7 (clone M-T701, Alexa700), CD123 (clone 6H6, Alexa700), CD11c (clone 3.9, Alexa700), CD20 (clone 2H7, PE-Cy5), IgA (goat polyclonal antibodies, APC), IgG (clone G18-145, BUV737), IgM (clone G20-127, BUV396), IgD (goat polyclonal antibodies, PE), CD80 (clone L307.4, BV786), CD95 (clone DX2, BV711), CD27 (clone M-T271, BUV563), CD21 (clone B-ly4, BV605), CD14 (clone M5E2, BV570) and CD138 (clone DL-101, PE-CF594).
Validation	mAbs were used according to manufacturer's instructions and previously published methods; mAbs were validated and titrated for specificity prior to use

Eukaryotic cell lines

Policy information about cell lines

Cell line source(s)	HEK293T and Vero E6 cells Commerically purchased (ATCC)
Authentication	Cell lines were not authenticated.
Mycoplasma contamination	Negative for mycoplasma

Commonly misidentified lines (See ICLAC register)	No commonly misidentified cell lines were used in the study

Animals and other organisms

Policy information about studies involving animals; ARRIVE guidelines recommended for reporting animal research

Laboratory animals	18 male and female cynomolgus macaques (Macaca fascicularis), 3-20 years old
Wild animals	None
Field-collected samples	None
Ethics oversight	All animal studies were conducted in compliance with all relevant local, state, and federal regulations and were approved by the Bioqual Institutional Animal Care and Use Committee (IACUC).

Note that full information on the approval of the study protocol must also be provided in the manuscript.